International Journal of Mineral Processing 102–103 (2012) 58–68

Contents lists available at SciVerse ScienceDirect

International Journal of Mineral Processing

journal homepage: www.elsevier.com/locate/ijminpro

Drainage and rupture of thin foam films in the presence of ionic and non-ionic surfactants

Liguang Wang *

The University of Queensland, School of Chemical Engineering, Brisbane, Qld 4072, Australia

ARTICLE INFO

Article history:
Received 8 April 2011
Received in revised form 12 September 2011
Accepted 25 September 2011
Available online 1 October 2011

Keywords:
Bubble coalescence
Surface forces
Film thinning
Film rupture
Surface mobility

ABSTRACT

The thin film pressure balance technique was used to determine the overall magnitude of the surface forces in foam films stabilized by flotation reagents such as sodium dodecyl sulfate and polypropylene glycol at high NaCl concentrations. The Stefan–Reynolds lubrication approximation was used to estimate the forces from measured film thinning rates while the capillary wave model of Valkovska, Danov and Ivanov was used to calculate the forces from measured critical rupture thicknesses. It was found that at very low surfactant concentrations commensurate with typical flotation reagent dosage, the overall forces were attractive and up to one order of magnitude stronger than the Lifshitz–van der Waals forces. The forces became smaller with increasing surfactant concentration. It was also found that the forces obtained from the capillary wave theory were indifferent to changes in film radii and surface mobility, in contrast to the Reynolds lubrication approximation. For comparison, other film drainage models considering film surface mobility and hydrodynamic corrugation were used to fit the present experimental thinning curves obtained at very low surfactant concentrations. They also showed that the overall attraction forces were several times stronger than the Lifshitz–van der Waals forces.

1. Introduction

Control of froth stability plays an important role in determining the product grade, throughput and recovery achieved from a flotation operation (Mathe et al., 1998; Neethling and Cilliers, 2003; Ata et al., 2003; Pugh, 2007). However, the froth phase in flotation has received little attention and has been recognized as "probably the most neglected phase in flotation research in stark contrast to its importance" (Nagaraj and Ravishankar, 2007). In modeling froth behavior, prediction of bubble coalescence and surface busting remains one of the most challenging tasks (Cillers, 2006).

Flotation froth is often generated using very low concentrations ($<10^{-4}$ M) of surfactants (frothers), in contrast to bubbles and foams (or froth) generated in many other industries using high surfactant concentrations close to the critical micelle concentrations (cmc). One of the most widely used non-ionic surfactants in flotation is methyl isobutyl carbinol (MIBC), and its dosage in flotation practice is low, usually in the range of 0.5- to 1.5×10^{-4} M. Besides MIBC, other commonly used flotation frothers include water-soluble polymers such as polypropylene glycols with molecular weights of 200 to 800. Polypropylene glycols are considered more powerful frothing agents than MIBC, and therefore lower dosages are usually applied (Klimpel, 1995). Ionic surfactants such as sodium dodecyl sulfate are used as both collectors and frothers in non-sulfide mineral flotation. These ionic surfactants also have frothing capability and can stabilize air bubbles in the froth phase of flotation. In addition to surfactants and polymers, salt water (or seawater) has also been used as frothing agent (Klassen and Mokrousov, 1963; Castro et al., 2010). Shortage of fresh water has driven some flotation plants to use salt water as frothing agent. Nevertheless, it is beneficial to use combined addition of inorganic electrolytes and surfactants (Yarar and Dogan, 1987). A fundamental understanding to this phenomenon is limited.

In this communication, we studied the drainage and rupture of single foam films containing sodium dodecyl sulfate in the presence of 0.3 M NaCl and polypropylene glycol with an average molecular weight of 400 (Dowfroth 400) in the presence of 0.1 M NaCl. The main component of the driving forces for film drainage and rupture, the inter-bubble attraction, was determined from film thinning kinetics by applying the film drainage model of Scheludko and Platikanov (1961) and from critical rupture thicknesses by applying the capillary wave model of Valkovska et al. (2002), respectively. For a given film, we compared the magnitudes of the overall surface forces obtained from film drainage and rupture. The effect of surface mobility on the magnitudes of the forces was also evaluated. The implication of these results on flotation was discussed.

2. Materials and experimental methods

Specially pure sodium dodecyl sulfate (SDS) was obtained from Fluka and recrystallized from ethanol. The polypropylene glycol (PPG) with an average molecular weight of 400 was also obtained from Fluka. Sodium chloride (99.5%, Sigma Aldrich, USA) was purified

* Tel.: +61 7 3365 7942; fax: +61 7 3365 4199.
E-mail address: L.Wang@eng.uq.edu.au.

0301-7516/$ – see front matter © 2011 Elsevier B.V. All rights reserved.
doi:10.1016/j.minpro.2011.09.012

by roasting at 700 °C for 5 h. De-ionized (DI) water (18.2 MΩ·cm^{-1}) used was produced by a Milli-Q unit (Millipore, USA) which was combined by a Reverse Osmosis system. All the glassware and the film holder were cleaned with concentrated sulfuric acid and vigorously rinsed with deionized water.

The static surface tension isotherm was measured at 22 °C using Wilhelmy plate method.

The TFPB technique developed by Scheludko and Exerowa (1959) was used to study the surface forces in the foam films. Inside a closed and vapor-saturated vessel, a single horizontal foam film was formed using a film holder, so-called Scheludko Cell. Fig. 1 demonstrated the schematic diagram of the Scheludko Cell, which was essentially a glass capillary tube with a small orifice connecting a side glass tube. The side glass tube, whose upper end was connected to a piston, was used to transport solution (or water). A single horizontal foam film is formed by sucking out the aqueous solution in the Scheludko Cell. Prior to experiments, it is important to make the inner wall of the film holder hydrophilic. Therefore, much effort has been made to clean the film holder. The inner radius (R_c) of the Scheludko Cell is 1.90 mm. The film radii (R_f) were controlled at 28–33 μm with measuring uncertainty of ±2.5 μm. It was observed that R_f remained unchanged during the course of film thinning. Special care was taken to ensure that no air bubbles are seen in the side glass tube filled with liquid, which is important for keeping R_f unchanged during film thinning. With a normal incidence light of wave length (λ), the thickness (H) of a homogeneous film with a refractive index (n_f) was determined interferometrically from the reflected light intensities using an optical equation (Scheludko, 1967):

$$H = \frac{\lambda}{2\pi n_f} \arcsin \sqrt{\frac{\Delta}{1+\frac{4R(1-\Delta)}{(1-R)^2}}} \quad (1)$$

where $\Delta = (I - I_{min})/(I_{max} - I_{min})$, $R = (n_f - 1)^2/(n_f + 1)^2$ with $n_f = 1.335$. In the above equation, λ is the wave length (equal to 546 nm in our case) and I_{max} and I_{min} are respectively the last maximum and minimum intensities of the reflected light from the film, while I is the instantaneous value of the reflected intensity during the thinning of the film.

The reflected light intensities (I) in Eq. (1) were estimated from the gray levels of the images of the films, according to a calibration curve. Although it is desirable to use a photomultiplier to directly measure the reflectance of the illuminated central zone of the films (Wang and Yoon, 2005), with the present microscope system this approach cannot be taken for very small foam films with radii below 50 μm. The calibration curve was made using several metastable foam films (R_f ~ 100 μm) at quasi-equilibrium. During calibration, the reflected lights from the film surfaces passed through a bandpass filter of 546 nm before reaching a photomultiplier, and the intensity of the monochromic (green) light was recorded. In what follows, the image of each film was taken on a different light path (free of bandpass filter) and processed offline to obtain the gray levels using the Vision Program of National Instruments. Fig. 2 shows a typical calibration curve. It demonstrates an excellent linear relationship ($R^2 = 0.9966$) between the digitized pixel gray level on the green plane of the images and the logarithm of the photomultiplier output, which follows the Weber's law (Weber, 1834). The calibration curve holds for films with different radii, i.e. 28–100 μm, where the gray levels of the images of a given film were observed to remain unchanged.

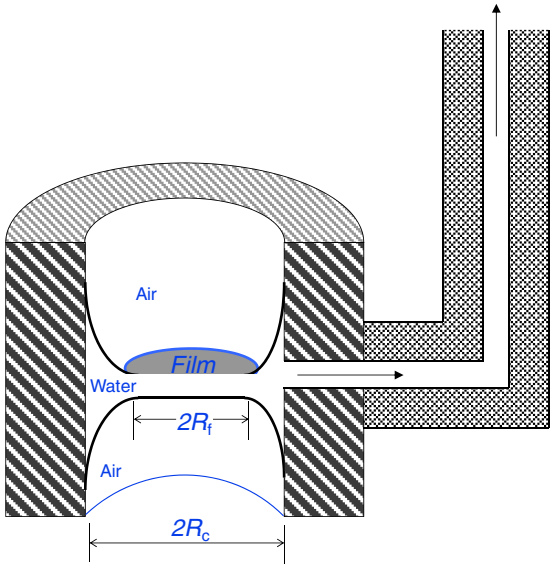

Fig. 1. Schematic diagram of the Scheludko Cell, a glass capillary tube with a small orifice connecting a side glass tube. A single horizontal foam film is formed in the capillary tube by sucking out the aqueous solution through the orifice.

3. Results

When a single horizontal foam film is formed in the Scheludko Cell (see Fig. 1), the driving force for the initial stage of film drainage is the capillary pressure (P_c). In the present work, the film radii (R_f) were controlled at 28–33 μm, which is significantly smaller than the inner radius, R_c, of the film holder, so the capillary pressure is given by the following equation (Scheludko, 1967; Exerowa and Kruglyakov, 1998):

$$P_c = \frac{2\gamma}{R_c} \quad (2)$$

where γ is the surface tension of the film-forming solution. Fig. 3 shows the surface tension isotherms for the frothers studied in the present work. The solid lines represent the Langmuir–Szyszkowski equation, $\gamma = \gamma_0 - RT\Gamma_m \ln(1 + K_L c)$ which has been fitted to the surface tension data, where γ_0 is the surface tension of pure water, R gas constant, T absolute temperature, Γ_m a maximum adsorption density, K_L the Langmuir equilibrium adsorption constant, and c the bulk concentration. For SDS, it gives 3.8×10^{-6} mol/m^2 for Γ_m, and 1.0×10^5 M^{-1} for K_L. The value of Γ_m for PPG is 1.0×10^{-6} mol/m^2, which is much lower than that of SDS. As is known, PPG has a larger molecular weight and hence a larger parking area than SDS. On the other hand, the value of K_L for PPG is 6.6×10^5 M^{-1}, which is higher than that of SDS.

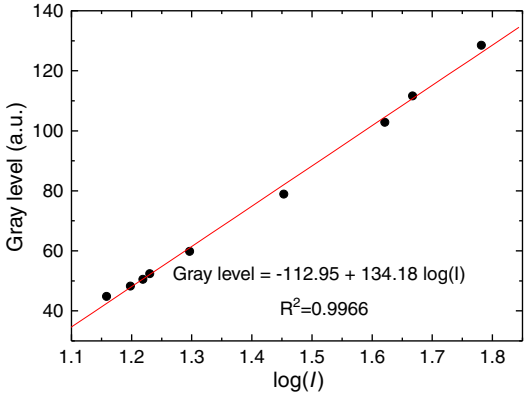

Fig. 2. Typical calibration curve between gray level of images and photomultiplier output (I).